mer, during which times sulfate is reduced (*15*). It is evident that detailed studies of sulfate input and annual variation are required in order to explain the scatter of these lake and brine data (*16*).

We have analyzed one sample of reagent $BaSO_4$ (*17*), which has a delta value of 6.87 ± 0.10 per mille; we cite this sample because its composition provides a useful standard for intercomparison of analytical results on sulfates. The further extension of this work clearly depends on laboratory measurements of exchange-rate constants and equilibrium fractionation factors; because of the many data now available on sulfur-isotope ratios, addition of data on another isotope in sulfates should provide important geochemical information on sulfates, as well as contributing to the possible development of another isotopic temperature scale.

A. LONGINELLI
H. CRAIG

Department of Earth Sciences and
Scripps Institution of
Oceanography, University of
California at San Diego, La Jolla

References and Notes

1. S. Epstein, R. Buchsbaum, H. A. Lowenstam, H. C. Urey, *Bull. Geol. Soc. Amer.* **64**, 1315 (1953).
2. A. Longinelli, *Nature* **207**, 716 (1965); **211**, 923 (1966).
3. E. R. S. Winter, M. Carlton, H. V. A. Briscoe, *J. Chem. Soc.* **1940**, 131 (1940); G. A. Mills, *J. Amer. Chem. Soc.* **62**, 2833 (1940); N. F. Hall and O. R. Alexander, *ibid.*, p. 3455; J. L. Hyde, *ibid.* **63**, 873 (1941); E. R. S. Winter and H. V. A. Briscoe, *J. Chem. Soc.* **1942**, 631 (1942); T. C. Hoering and J. W. Kennedy, *J. Amer. Chem. Soc.* **79**, 56 (1957); A. E. Brodsky, *J. Chim. Phys.* **55**, 40 (1958).
4. R. V. Teis, *Geochemistry USSR English Transl.* **1956**, 257 (1956).
5. J. Halperin and H. Taube, *J. Amer. Chem. Soc.* **74**, 375 (1952).
6. T. A. Rafter, *New Zealand J. Sci. Technol. B* **38**, 955 (1957).
7. H. Craig and A. Longinelli, in preparation.
8. The delta units are defined by $R/R_{SMOW} = (1 + \delta)$, where R is the ratio $O^{18} : O^{16}$ and SMOW is the defined standard mean ocean-water isotopic standard [H. Craig, *Science* **133**, 1833 (1961)], which is very close to the true oceanic mean. The delta values are expressed in per millage. Water samples are analyzed by equilibrating CO_2 with the water and by analyzing the CO_2; the analytical precision ($2\ \sigma$) is within 0.04 per mille. Carbon dioxide from sulfate is measured relative to CO_2 in equilibrium with SMOW at 25°C; in converting the sulfate data to delta values versus SMOW itself, as given in the tables, the fractionation factor (25°C) between CO_2 and H_2O was taken as 1.0407 [J. O'Neil and S. Epstein, *J. Geophys. Res.* **71**, 4955 (1966)].
9. Distilled water, used for dilution and washing, analyzed —9.0 per mille; in one instance (from the Marianas Trench sample) a duplicate portion was diluted and the precipitate washed with enriched water of $\delta = +45$ per mille. The resultant sulfate analyzed + 9.84, or 0.25 per mille heavier, indicating that not more than 0.5 percent of the water oxygen can appear in the final CO_2, and that the error from such oxygen is less than 0.1 per mille. In another experiment we precipitated only 10 percent of the sulfate in a sample and found the precipitate to be 1 per mille lower in oxygen-18 than the total sulfate.
10. H. Craig and L. I. Gordon, in *Stable Isotopes in Oceanographic Studies and Paleotemperatures*, E. Tongiorgi, Ed. (Consiglio Nazionale delle Richerche, Rome, 1965), pp. 9–130.
11. D. A. Livingstone, *U.S. Geol. Surv. Profess. Papers 440-G* (1963), pp. 40–41. About half the river sulfate might be "recycled," but the calculation is not sensitive to factors of 2. We have assumed here that input of sulfate by oxidation of H_2S within the sea is not significant, but this point needs some further study.
12. H. Craig, in *Earth Science and Meteoritics (F. G. Houtermans Volume)*, J. Geiss and E. Goldberg, Eds. (North-Holland, Amsterdam, 1963), pp. 103–114. The water residence times relative to mixing are much longer than the carbon residence times in such a model because carbon exchanges rapidly with the atmosphere.
13. H. Craig, *Science* **154**, 1544 (1966). The Red Sea brine samples in Table 1 of this present report are the samples described in this reference.
14. Y. K. Bentor, *Geochim. Cosmochim. Acta* **25**, 239 (1961).
15. L. H. Carpelan. *Calif. Dept. Fish Game Fish Bull.* **113**, 17 (1961).
16. H. C. Urey [*J. Chem. Soc.* **1947**, 562 (1947)] has calculated theoretical sulfate isotopic enrichments relative to liquid water of 19.4, 14.7, and 5.0 per mille at 0°, 25°, and 127°C, respectively. Although many of the lake and brine samples show enrichments in this range, we consider it much more likely that ocean-water sulfate ions are close to equilibrium with water, and that the calculated values are too high because of the many uncertainties in calculation of partition-function ratios for dissolved ions by treating them as perfect gases.
17. Baker and Adamson "Reagent $BaSO_4$"; 99-percent minimum purity. Our yields range from 92 to 100 percent, the low figures reflecting absorption of moisture during weighing.

18. Supported by NSF grants NSFgp-3347 and NSFga-351, and by ONR grant NONR-2216(23). A.L. was on leave from Laboratorio Geologia Nucleare, Pisa, while the work was done. We thank P. Kroopnick, S. Drais, and B. Hom for aid with the analyses. M. Lloyd has obtained similar data on ocean-water sulfates; we thank him for discussion.

21 November 1966

■

Rapid Methods of Determining Cooling Rates of Iron and Stony Iron Meteorites

Abstract. *Two rapid and simple methods have been developed for determining the approximate cooling rates of iron and stony-iron meteorites in which kamacite formed by diffusion-controlled growth along planar fronts. The first method requires only measurements of the mean kamacite bandwidth and the bulk nickel content. The second method requires the determination of the nickel composition near the taenite-kamacite interface with an electron microprobe.*

Recently we have developed (*1*) a method for determining the cooling rate of meteorites with Widmanstätten structure (octahedrites and pallasites). This structure formed within the temperature range of 700° to 300°C as the meteorite cooled within a parent body. The method is more precise (±10 to 40 percent) than previous calculations of cooling rates (*2*), but is complicated to apply because it involves the comparison of a complex computer calculation with nickel diffusion gradients in carefully selected and oriented kamacite and taenite bands. We have therefore developed two simplified methods for determining the cooling rates (at 500°C) of meteorites exhibiting Widmanstätten structure.

Kamacite (α) and taenite (γ) in iron meteorites are essentially Fe-Ni solid solutions containing, respectively, 5 to 7.5 percent and 15 to 50 percent Ni by weight. As the meteorite cooled through the temperature range 700° to 300°C, α phase nucleated in γ phase and grew by solid-state diffusion. The α plates form the unique pattern called the Widmanstätten structure. At lower temperatures decreasing diffusion rates caused compositional zoning next to the borders of taenite and kamacite. These can be easily measured with an electron microprobe (*1–3*).

The complex method (called hereafter the precise method) which we have developed (*1*) for determining the cooling rate of the Widmanstätten structures uses the known phase equilibria and diffusion coefficients in the Fe-Ni system. It also takes into account all the following factors which influence the formation of the Widmanstätten structure: (i) the bulk nickel content of the meteorite; (ii) undercooling below the equilibrium α-precipitation temperature; (iii) impingement of neighboring kamacite plates; (iv) the cooling rate of the meteorite; (v) pressure. Goldstein and Ogilvie (*2*) have shown that the pressure at the positions of the iron meteorites within the parent bodies was apparently not sufficient (< 10 kb) to influence the growth of kamacite. The other factors (i to iv) determine the ultimate kamacite bandwidth and the shape of the retained diffusion gradients in both taenite and kamacite. This method, as well as the two described below, also assumes that minor elements in the meteorite have not significantly affected either the diffusion coefficients of nickel or the Fe-Ni phase equilibria dur-

Table 1. Maximum Ni content in taenite ($C_{\gamma\text{-max}}$) and minimum Ni content in kamacite ($C_{\alpha\text{-min}}$), as measured by electron microprobe at 20 kev next to taenite-kamacite borders in iron meteorites and pallasites, listed in order of decreasing cooling rate (*1*).

Meteorite	Cooling rate at 500°C (°C/10^6 yr)	γ/α Boundary compositions (% Ni by wt.)	
		Edge of γ	Edge of α
Bristol	20	34	6.8
Gibeon	20	35	6.5
Altonah	20	36	6.8
Duchesne	9	34	6.9
Dayton	6.5	38	6.5
Grant	5.1	37	6.6
Carlton	4.2	37	6.4
Woodbine	2.7	43	5.6
Tazewell	2.2	43	5.6
Edmonton	1.9	40	6.0
Four Corners	1.9	43	5.9
Toluca	1.6	43	5.8
Giroux	1.3	45	5.5
Carbo	1	45	5.8
Newport	1	47	5.5
Mount Vernon	0.8	48	5.2
Imilac	.5	48	5.3
Butler	.5	48	5.3
Brenham	.5	48	5.4
Glorieta	.5	49	5.5
Albin	.5	49	5.4
Springwater	.4	49	5.5

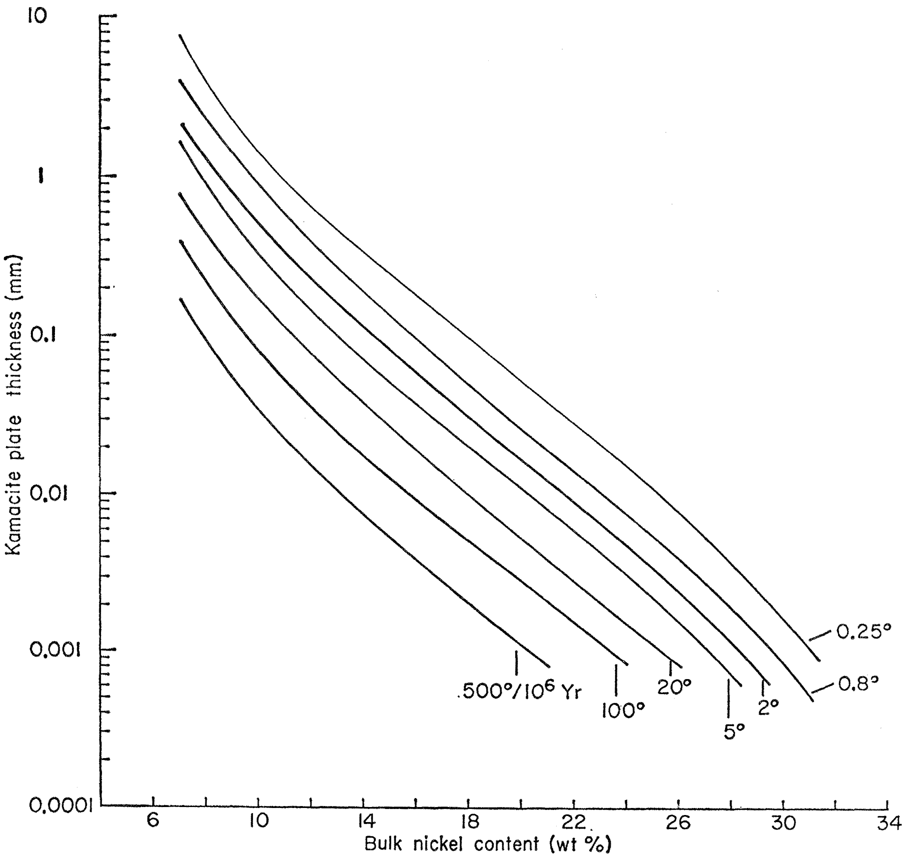

Fig. 1. Cooling rate (±100 percent) of Widmanstätten structure of 500°C as a function of kamacite plate thickness and bulk Ni content of metallic phase of meteorite. The nucleation temperature of kamacite is taken to be 110°C below the $\gamma/(\alpha+\gamma)$ boundary in the Fe-Ni phase diagram (*4*), and it is assumed that kamacite growth is unimpeded by other impinging kamacite plates.

ing growth of the Widmanstätten structure. Using these assumptions, we are indeed able to match exactly the observed diffusion gradients and kamacite plate thicknesses to those calculated for a unique cooling rate.

Method 1. The basis for the first approximate method lies in assuming values for undercooling and impingement, thus permitting the cooling rate to be obtained simply by measurement of bulk nickel content and mean kamacite plate thickness. In 27 meteorites studied by the precise method it was found that α must have nucleated only after undercooling below the $\gamma/(\alpha + \gamma)$ boundary in the Fe-Ni phase diagram (*4*). The extent of this undercooling was found to be consistently 110° ± 15°C in 90 percent of the largest kamacite plates which form the Widmanstätten structure. No significant differences in undercooling were found between different groups of meteorites or between meteorites with different cooling rates or nickel content.

The impingement factor is related to the coarseness of the Widmanstätten structure. It is negligible in meteorites with fast cooling rates or high bulk nickel content. In ataxites and many octahedrites of fine structure the diffusion gradients in γ phase do not extend to the center of the taenite. In meteorites with low bulk nickel content and coarse structure, the impinging diffusion gradients increase the central nickel content of taenite above the original composition. In medium octahedrites and to a lesser extent in coarse octahedrites the influence of impinging diffusion gradients which move toward each other is to increase greatly the central nickel contents of the taenite bands. However, even in coarse octahedrites the impingement influences the ultimate thicknesses of the kamacite plates much less than it does the shape of the gradients within taenite. Moreover, 80 percent of the growth of the Widmanstätten structure occurs in the first 50°C of cooling after nucleation during which diffusion rates are fastest but impingement is insignificant. In effect, except for the coarsest octahedrites, the largest kamacite plates nucleated far enough apart that their growth did not seriously interfere with one another.

On the basis of the above considerations, computer calculations of the α plate thickness were made as a function of cooling rate (normalized to 500°C) and bulk nickel content, assuming undercooling of 110°C below the $\gamma/(\alpha + \gamma)$ boundary in the Fe-Ni phase diagram (*4*), and assuming no impingement. A graph (Fig. 1) of kamacite plate thickness versus bulk nickel content was then obtained for various cooling rates. To test the effect of the approximations, we measured the average bandwidths on etched sections of iron meteorites on which precise cooling rates had been determined (*1*). At least ten bands were measured on each meteorite, either on photomicrographs or microscopically with a calibrated eyepiece micrometer. The kamacite bands selected were major bands which establish the gross Widmanstätten structure and have a bandwidth variation of less than ± 20 percent. Inclusions such as schreibersite were avoided. The band system chosen intersects the section surface at a steep angle. The measured kamacite bandwidths were related to plate thickness by determining the dip-angle of the plates by angle measurements on the top surface and a second perpendicular surface (see, for example, *5*).

The percentage deviations between approximate method 1 and the precise method for determining the cooling rate were calculated. Their standard deviation is ± 50 percent. However, the mean percentage deviation between the two methods is only −2 percent for the 18 meteorites studied, showing that no significant positive or negative bias is introduced by the approximations to the precise theory.

Method 2. The basis for the second approximate method lies in calculating the effect of variation in cooling rate on the diffusion gradients near the kamacite-taenite border. Theoretically, the compositions at the interface of kamacite and taenite represent the equilibrium compositions at the lowest temperature at which equilibrium was maintained. However, the true interface compositions cannot be measured with the electron microprobe because of the finite size of the x-ray excitation volume. Across a typical area of x-ray excitation 2 μ in diameter (at 20 kev) the diffusion gradient might extend from 30 to 50 percent Ni, and only an average composition could be measured. A similar situation, but with a shallower gradient, prevails in kamacite.

Nevertheless, the maximum nickel content measured in taenite ($C_{\gamma\text{-max}}$), the minimum nickel content measured in kamacite ($C_{\alpha\text{-min}}$), and the cooling rate are correlated (Table 1). Meteorites with known cooling rates (*1*) were found to have proportionally higher average values of $C_{\gamma\text{-max}}$ and lower average values of $C_{\alpha\text{-min}}$ for decreasing cooling rates. We measured $C_{\gamma\text{-max}}$ and $C_{\alpha\text{-min}}$ on sections cut perpendicular to the kamacite plates. $C_{\gamma\text{-max}}$, which can be measured with ±4 percent relative accuracy, is more sensitive to changes in cooling rate than $C_{\alpha\text{-min}}$. An ARL electron microprobe with an approximate x-ray excitation diameter of 2 μ at 20 kev was used. Under these operating conditions a least squares fit of $C_{\gamma\text{-max}}$ and cooling rate conforms to the equation

$$\log_{10} \text{(cooling rate)} = 4.77 - 0.104\ C_{\gamma\text{-max}}$$

This relation varies with different excitation conditions. Therefore, in order to use this method for determining cooling rates, for the electron probe used it is advisable to calibrate $C_{\gamma\text{-max}}$ with meteorites of known cooling rate (for example, those in Table 1). The kamacite plates chosen should intersect the top surface at or near 90° in order to avoid errors in $C_{\gamma\text{-max}}$ and $C_{\alpha\text{-min}}$ from subsurface effects.

Method 1 is recommended for meteorites showing good Widmanstätten structure. It has better precision for medium and fine octahedrites and ataxites than for coarse octahedrites and cannot be used for hexahedrites. When the cooling rates are fast and the gradients steep and hard to measure, method 1 is probably more accurate than the precise method. Method 2 supplements method 1 in such cases as pallasites which have kamacite plates in which kamacite grew by planar-front diffusion. It becomes imprecise when the cooling rate is greater than 50°C/10^6 years, owing to the steepness of the gradient, or when impingement raises the central taenite nickel content over 20 percent by weight, thus flattening the gradient near the α/γ interface. With these restrictions both approximate methods can much more rapidly and easily give cooling rates within ±50 percent of those obtained by the precise method.

JAMES M. SHORT*
Space Sciences Division,
Ames Research Center,
Moffett Field, California 94035
JOSEPH I. GOLDSTEIN
Geochemistry Laboratory,
Goddard Space Flight Center,
Greenbelt, Maryland 20771

References and Notes

1. J. I. Goldstein and J. M. Short, *Geochim. Cosmochim. Acta*, in press.
2. J. I. Goldstein and R. E. Ogilvie, *ibid.* **29**, 893 (1965); J. A. Wood, *Icarus* **3**, 429 (1964).
3. J. M. Short and C. A. Andersen, *J. Geophys. Res.* **70**, 3745 (1965); J. I. Goldstein, *ibid.*, p. 6223; S. J. B. Reed, *Geochim. Cosmochim. Acta* **29**, 535 (1965).
4. J. I. Goldstein and R. E. Ogilvie, *Trans. AIME* **233**, 2083 (1965).
5. C. M. Nevin, *Principles of Structural Geology* (Wiley, New York, 1949), p. 346.
6. Klaus Keil graciously provided electron microprobe facilities for part of the experimental work. One of us (J.M.S.) was supported by a National Academy of Sciences Resident Research Associateship at the Ames Research Center.

* Present address: U.S. Geological Survey, Menlo Park, California 94025.

24 February 1967

Amphibole: First Occurrence in a Meteorite

Abstract. *This is the first report of an amphibole mineral found in any meteorite. The amphibole richterite (soda tremolite),* $Na_2Ca(Mg,Fe)_5Si_8O_{22}(OH,F)_2$, *occurs as a primary (preterrestrial) mineral enclosed within graphite nodules in the iron meteorite from Wichita County, Texas.*

No member of the amphibole group of silicates, which is quite prominent in terrestrial rocks, has, until now, been found in any meteorite. I now report the finding of the amphibole, richterite (soda tremolite) in the iron meteorite from Wichita County, Texas. The x-ray powder-diffraction pattern is compared with that of a richterite from Langban, Sweden, in Table 1.

The mineral was analyzed by electron microprobe (*1*) and the results are given in Table 2. The microprobe could not, of course, provide a direct analysis of hydroxyl, nor is a direct analysis by chemical methods possible on the microgram quantities present. Similarly the small quantities also preclude determination by infrared absorption methods. Since terrestrial richterites are known to have as much as 62 percent (atom) of the hydroxyl position substituted by fluoride (*2*), a direct analysis of F was made. In addition, the mineral was analyzed for Cl, Br, and I but none were found (that is, less than 0.1 percent by weight). The analysis was then normalized to eight Si atoms. The fluoride thus calculated was 0.996 atoms (rounded to 1.00) and the remainder of the hydroxyl position was filled with OH (that is, OH = 1.00), which was then calculated to H_2O and added to the probe analysis (Table 2). During the microprobe work it was observed that there was a modest variation in Cr from grain to grain (by a factor of 1.5 from lowest to highest value) and a larger variation in Ti (by a factor of almost 1.9). The values reported in this analysis are based on the average of the counts observed. These are not major elements; however, it is suspected that their variability is causing the small variation in optical properties. Optical parameters are: biaxial, negative; weak dichroism (X, pale blue-green; Z, brown); 2V = 40 to 60°; α = 1.598 to 1.607; β = 1.616 to 1.625; and γ = 1.621 to 1.628 (values ± 0.002).

The richterite was collected by excavating into nodules of graphite. The grains are small (the largest is 0.6 by 0.2 mm), are found near the centers of the nodules, and are completely enclosed by graphite. They occur immediately adjacent to clear, colorless olivine grains (forsterite 99). In addition the nodules contain albite (Ab 99), roedderite (*3*), and whitlockite, along with an unidentified phosphate and an unidentified silicate. In addition to the graphite nodules, separate troilite nodules occur which contain isolated specks of sphalerite, diopside, and orthorhombic enstatite.

The presence of a hydroxyl-bearing amphibole in an iron meteorite at first